International Journal for Modern Trends in Science and Technology, 9(03): 248-255, 2023

ISSN: 2455-3778 online
DOI: https://doi.org/10.46501/IJMTST0903038
Available online at: http://www.ijmtst.com/vol9issue03.html

High Step Up Transformerless DC-DC Converter Designed for Use in Applications Involving Renewable Energy

Chandu Challa, Bommireddy Kumar Naidu, Shubham Kumar, Dr. V Suresh

Department of Electrical Engineering, Godavari Institute of Engineering and Technology(A), Rajahmundry, A.P, India.

To Cite this Article
Chandu Challa, Bommireddy Kumar Naidu, Shubham Kumar and Dr. V Suresh. High Step Up Transformerless DC-DC Converter Designed for Use in Applications Involving Renewable Energy. International Journal for Modern Trends in Science and Technology 2022, 9(03), pp. 248-255. https://doi.org/10.46501/IJMTST0903038

Article Info
Received: 28 February 2023; Accepted: 18 March 2023; Published: 19 March 2023

ABSTRACT

Switch-mode power supply, fuel cells, and solar photovoltaic systems are just some of the many places you'll find a high gain dc-dc converter in use. We present a dc-dc boost converter with a record-breaking gain and do considerable research on it. The proposed setup may achieve significant voltage gain compared to previous transformerless designs. As long as the output voltage doesn't go beyond 50%, the active MOSFETs are safe. We settle for the lowest-rated components because of this. The underlying operational logic of both systems is dissected to establish their respective benefits. The converter's performance is deemed satisfactory both in open and closed loop configurations, and high gain is attained at low duty ratios.

KEYWORDS: Boost converter, ultra high gain, , duty cycle, , voltage stress, DC microgrid

1. INTRODUCTION

Power electronics are an essential component in the effort to get the maximum amount of energy from sources that are both sustainable and kind to the environment. Figure 1 presents a schematic representation of a DC microgrid. High gain dc-dc converters act as a mediator between the load and the source, taking the relatively low DC voltage (12V-60V) supplied by the battery, solar photovoltaic (PV), or fuel cell and increasing it to practical levels (200-300V). In addition, a DC microgrid equipped with a high gain dc-dc converter maintains the voltage of the dc connection at the level that has been established [1]. In today's current DC microgrids, it is common practise to combine supercapacitors and high gain dc-dc converters. This is due to the fact that supercapacitors have a high power density but a low voltage rating. In today's market, rapid charging at level three often makes use of high-gain converters for electric cars (EV). AC loads may be served by a DC microgrid that is operating in islanded mode by combining a high gain converter with an inverter. This allows for the microgrid to run independently. High gain converters have lately come into prominence as an alternative to traditional boost converters and its variants [1], which are characterised by their poor efficiency and high duty cycle operating requirements. At addition to that, there is the problem of diode reverse recovery in higher duty cycles.

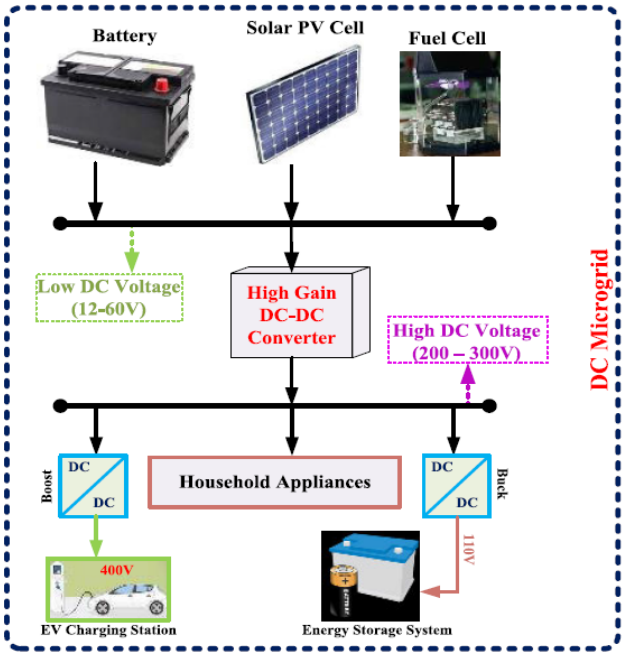

Fig 1.Simple schematic of DC microgrid.

In theory, a conventional boost converter's voltage gain may approach infinity under optimal conditions. However, in practise, its capability to step up is limited by conduction losses resulting from resistances and diode voltage drops, as well as by the parasitic components of the power device, such as capacitance and inductance. Reverse recovery may be hindered by a high step-up ratio, and magnetic saturation may occur if the power switch is tripped during the high duty cycle [2-5]. Multiple papers [2–14] offer research into the development of high-efficiency, high-gain boost converters. Step-up dc/dc converters may be categorised in part based on whether or not the transformer inside of it is isolated. If the turns ratio is optimised, transformer-based topologies may achieve high voltagegain. Separating the input circuit from the output circuit, transformers play a crucial role. Transformer-free topologies have analogous costs, weights, and degrees of complexity [12]. However, the switching devices in the cascading boost converter design given in [14] are vulnerable to high voltage/current stress as the architecture enables more voltage gain without an excessive duty cycle compared to the conventional boost converter. Using switching inductors and capacitors is another possible method for increasing the voltage gain [15-19]. Switched inductor converters have double the voltage gain of regular boost converters, while subjecting their semiconductors to far higher voltages. Several papers [20-22] have utilised the voltage lift approach to produce a significant voltage boost while reducing the voltage and current load on switches. However, more diodes and capacitors are required when the conversion ratio is large. When controlling the voltage gain of a converter with an isolated topology like linked inductors or a flyback converter, the turns ratio is employed in addition to the duty cycle. Achieving the necessary step-up ratio with a reasonable duty cycle is essential for improving overall efficiency. On the other hand, when energy is released from leaky inductance in topologies like the flyback converter, voltage spikes arise on the active switch. Energy is wasted and dissipation is increased due to the leaky inductance of the active switch [22, 23]. Passive clamp circuits [23, 24] and active clamp circuits [25, 26], both of which may be regarded costly at times, are two examples of techniques that can be used to cope with issues of this nature. Voltage may be increased using switched capacitor converters without the need of any magnetic parts [25-28]. It is mentioned in [29] that the efficiency of hard-switching switched capacitor boost converters is less than 75%. Switched capacitors may function better with an additional resonance inductor [29,30]. The boosting range is still limited in comparison to inductor-based converters, where the duty cycle may be adjusted to provide a large range of boosting. The input voltage may range from 33 V to 45 V when the PV module is connected directly to the dc-dc converter in these scenarios, necessitating a large step-up capability of the converter. The dc-dc converter's main job is to boost the module's voltage to a level that's higher than 3350 V but lower than 400–700 V. That's why it's so important to have a robust step-up skill set. As part of this study, a novel high-performance dc/dc converter is introduced. Numerous systems, including photovoltaic (PV) ones, might benefit from the suggested converter. The proposed design has various benefits, including a good step-up capacity, low voltage stress on the active components, and acceptable efficiency. There are three main components that make up the framework of this piece. The next part of this article will include some steady-state research and a discussion of the suggested converter's functionality. The experiments and their results are presented in Section 3. Part 4 includes the conclusion and a brief review of the preceding chapters.

2. PROPOSED HIGH GAIN CONVERTER

The suggested converter's configuration is shown in Fig. 2. It has three diodes, three inductors, one capacitor, and three switches. As a result of a single trigger, all three switches and diode D2 turn on and off simultaneously. Similar to how the switches work, the two additional diodes provide a complementary function. When the switches are on, the inductors store energy and release it to the output load when the switches are off. The small-ripple approximation will be used in the subsequent investigation. In addition, the converter was developed to run in a mode where conduction occurs constantly. To simplify the study of the converter, we will assume that the parameters are optimal in the future. In Fig.3, we see a graph depicting the optimal waveforms for the circuit's essential components. Depending on which switches are engaged, the converter may function in either of two modes.

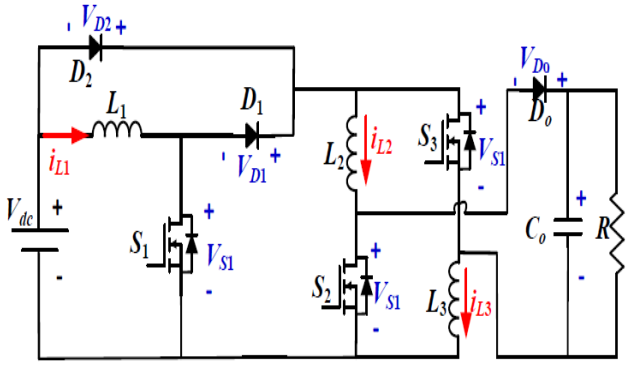

Fig.2. proposed configuration

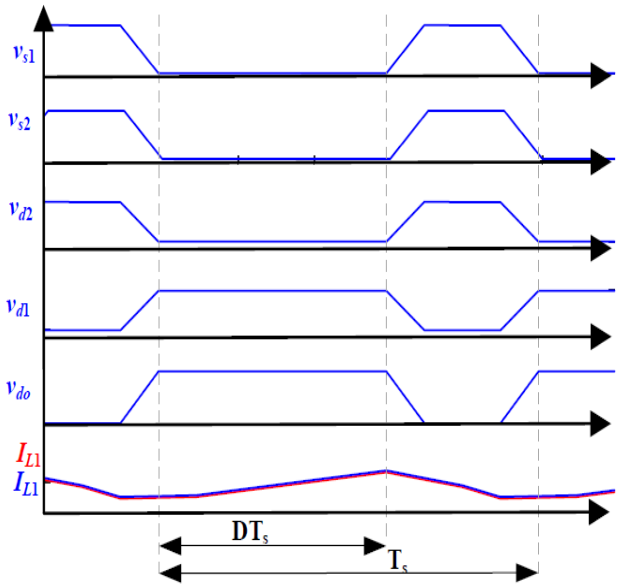

Fig.3. Ideal key waveforms

Mode I

When the switches are switched on, the system enters this state, which is seen in Fig. 4. At the same moment, all three switches and diode D2 are activated. All three inductors (L1, L2, and L3) are charged from the input dc-source in this configuration. As a result of the voltage being inverted across diodes D1 and Do, they are disabled. The output capacitor Co is releasing its charge into the load. The defining equations for this operational mode are as follows:

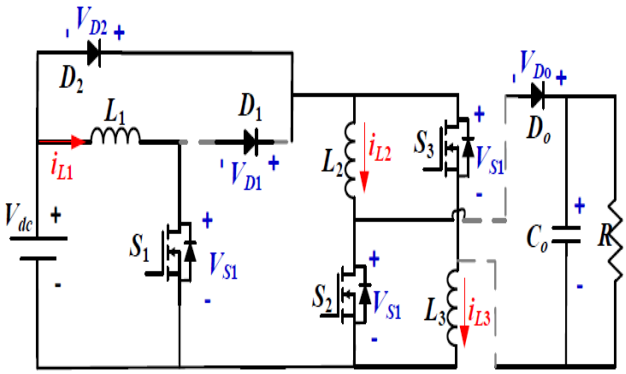

Fig.4. Configuration of Mode I

$$\begin{cases} v_{L1}(t) = v_{L2}(t) = v_{L3}(t) = V_{in} \\ i_{co}(t) = -V_o/R \end{cases} \quad (1)$$

Mode II

Once the switches are switched off, the system enters this state, which is seen in Fig. 5. There is a simultaneous shutoff of all three switches. As a result, power from inductors L1, L2, and L3 is being transferred to the output load and output capacitor Co. Turning on diodes D1 and Do makes them function as a freewheeling diode, maintaining a continuous channel for the inductor currents. The defining equations for this operational mode are as follows:

$$\begin{cases} v_{L1}(t) = v_{L2}(t) = v_{L3}(t) = (V_{in} - V_o)/3 \\ i_{co}(t) = i_L - V_o/R \end{cases} \quad (2)$$

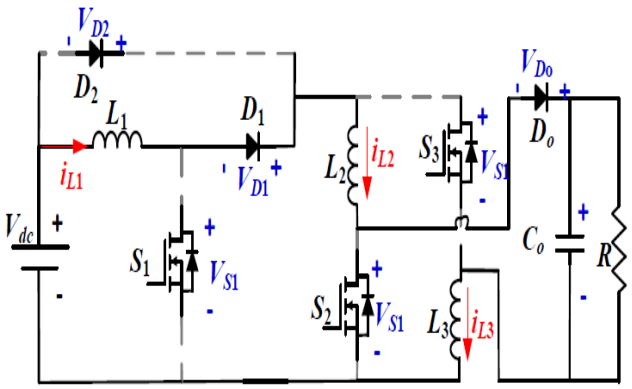

Fig.5. Configuration of Mode II.

$$\frac{V_o}{V_{in}} = \frac{2(1+D)}{(1-D)} \qquad (3)$$

The relation between output and input voltage may be calculated using eq (1) and eq (2) [18], provided that the inductor and capacitor are charged in a balanced manner.

The converter's voltage gain may be calculated using the following (3). Values for the input voltage, the output voltage, the voltage across capacitor C1, the duty cycle, the load resistance, the voltage across inductor L1, the voltage across inductor L2, the current through capacitor Co, the current across inductor L1, and the current across inductor L2 are indicated by the symbols Vin, Vo, VC1, D, R, vL1, vL2, ico, il1, and il2.

In Table II, we can see the effects of the high voltage on each part. All of the parts are subjected to stress voltages that are less than the final output voltage. For this reason alone, this topology is preferable. Selecting a device with a lower power rating increases the system's efficiency.

The amount of ripple in the inductor current and capacitor voltages is taken into account while designing the circuit's parameters. A low current ripple in the inductor is essential for continuous-current-mode functioning. The ensuing sections detail the design of each individual part of the circuit. Figure 6 shows the stress placed on components due to voltage changes at varying voltage gains. This illustration uses an input voltage of 50V. The output diode takes the brunt of the voltage stress, whereas diode D1 maintains a constant voltage independent of the converter's voltage gain.

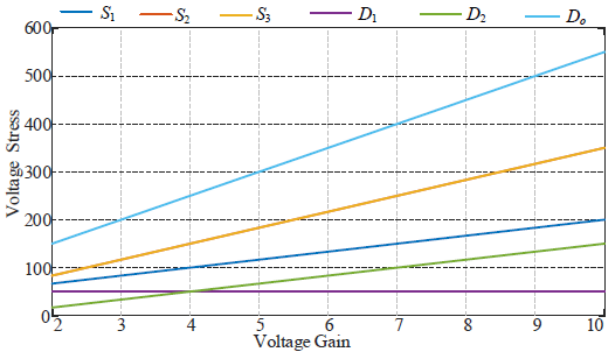

Fig.6. Component voltage stress at different voltage gain and input voltage 50V

3. Parameters Design

Inductor L1 design

It is shown in Fig.7 as a rough drawing of the current in the inductor. First, let's calculate the first subinterval's change in inductor current,, which is given by the formula:

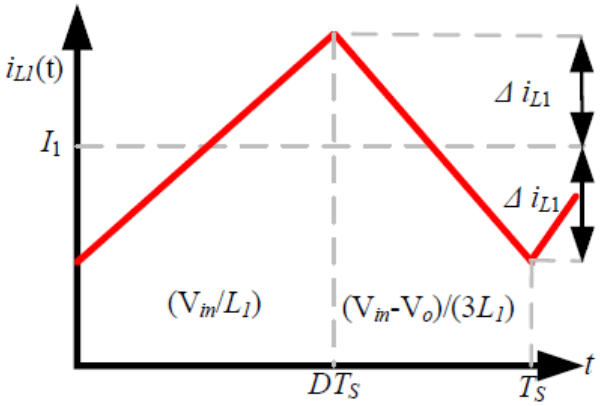

Fig.7. Inductor *L*1 current

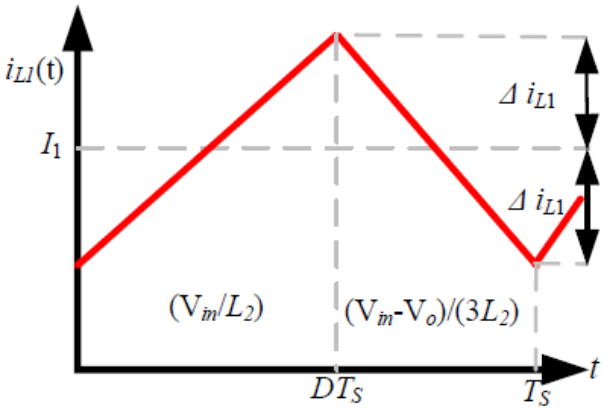

Fig.8 Inductor *L*2 and *L*3 currents.

$$2\Delta i_{L1} = \left(\frac{V_{in}}{L_1}\right) DT_S \quad (4)$$

$$L_1 = \left(\frac{V_{in}}{2\Delta i_{L1}}\right) DT_S \quad (5)$$

The value of the inductor L1 is chosen with the help of Equation (5). The input voltage Vin, duty cycle D, sampling time TS, and inductor current ripple all affect the value of inductor L1.

Inductor L2 &L3 design

Fig.8 is a diagram depicting the current via an inductor. First, let's calculate the first subinterval's change in inductor current,, which is given by the formula:

$$2\Delta i_{L2} = \left(\frac{V_{in}}{L_2}\right)\left(\frac{DT_S}{1-D}\right) \quad (6)$$

$$L_2 = L_3 = \left(\frac{V_{in}}{2\Delta i_{L2}}\right)\left(\frac{DT_S}{1-D}\right) \quad (7)$$

Output capacitor Design Co

In a similar vein, an equation may be obtained for the peak magnitude of the output voltage ripple by sketching the voltage waveform across the capacitor. Fig.9 shows a representation of the voltage waveform across the capacitor. The voltage shift across the capacitor, denoted by vo, is proportional to the slope times the subinterval duration.

$$\Delta v_o = \left(\frac{V_o}{2RC_o}\right) DT_S \quad (8)$$

$$C_o = \left(\frac{V_o}{2\Delta v_o C_o}\right) DT_S \quad (9)$$

The value of the output capacitor is chosen using (9). The output voltageVo, duty cycleD, sampling timeTs, and capacitor voltage ripple all play a role in determining its value.

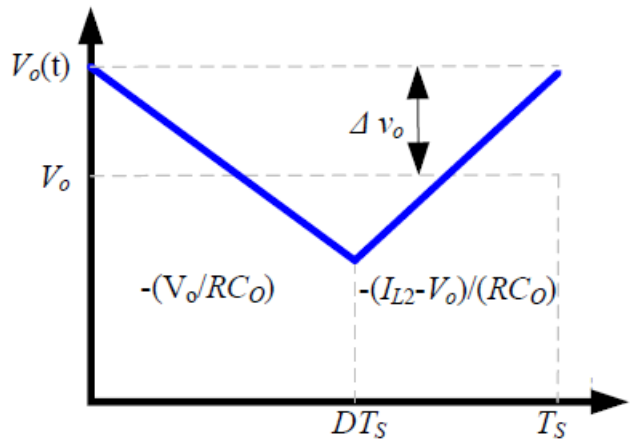

Fig.9. Capacitor *Co* voltage.

Components of the circuit and the voltages they are subjected to are listed in Table 1. Voltage stresses on the switches are less than the output voltage, on diode D1 they are equal to the input voltage, and on diode D2 they are less than a third of the output voltage. In most boost converters, the output diode Do is the sole circuit element subjected to high voltage stress.

Table1: TopologyVoltage Stresses

Device	Voltage stress
S_1	$(V_o+2V_{in})/3$
S_2	$(2V_o+V_{in})/3$
S_3	$(2V_o+V_{in})/3$
D_1	V_{in}
D_2	$(V_o-V_{in})/3$
D_o	V_o+V_{in}

4. Results and Discussion

The suggested converter has been tested, and the experimental findings based on the laboratory prototype confirm its effectiveness. Table 2 lists the converter settings that will be used in the proposed system. Lab prototype shown in Fig. 9.

Table 2: Specification of design parameters

V_{in}	Input Voltage	20-40V
V_o	Output Voltage	200-450
L_1, L_2	Input Inductor	3 *mH*
C_{in}	Input Capacitor	260 µF
C_1	Parallel capacitor	260 µF
C_o	Output Capacitor	260 µF
S_1 and S_2	Power Mosfet	*IRFP*264
D_1, D_2	Power Diode	*BYV72EW*-200
D_o	Output Diode	*BYV72EW*-200
F_S	Switching Frequency	10 KH_Z
P_o	Output Power	150 *W*

All three of the converter's switches are turned on and off at the same time. You can see the pulses being applied to the gate-source of the three MOSFETs. Applying symmetrical pulses to the three switches causes them to all operate at once. Switches S2 and S3 are under about the same amount of voltage stress as one another, whereas switch S1 is under far less.

There are three diodes in this topology. Diode D1 and the power MOSFETs are both active at the same time, while diodes D2 and Do work in parallel to provide a shunt for the inductor current.

High voltage gain and moderate efficiency are both desirable in converters used in renewable energy applications. High voltage gain and maintaining a modest efficiency are both desirable in converters used in renewable energy applications. The calculated and theoretical voltage gains are shown in Fig. 10. Copper losses and on-resistance of the MOSFETs contribute to the discrepancy between the observed and ideal voltage gain. At 20 V input voltage and 0.7 duty cycle, the efficiency of the system is assessed at a variety of power levels up to 200 W. As can be seen in Fig.11, the converter achieves an efficiency of almost 90%.

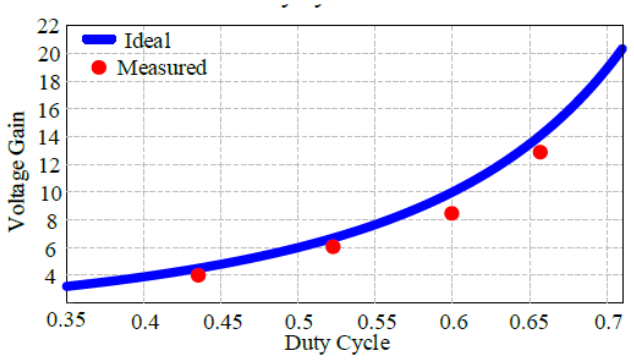

Fig.10. Ideal and measured voltage gain

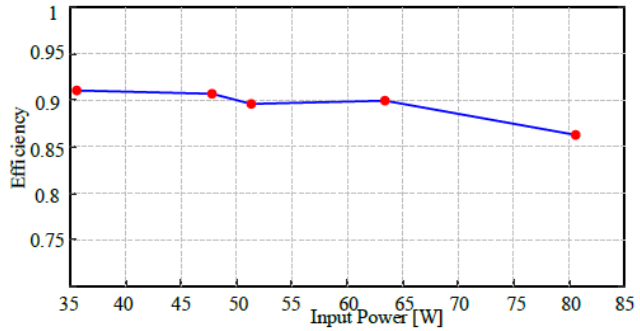

Fig.11. Measured efficiency

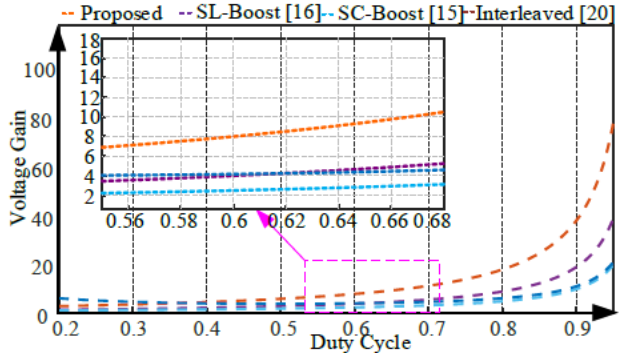

Fig.12. Voltage gain comparison among different dc-dc step up topologies

Integration of PV systems into preexisting infrastructure is a common problem with a number of published solutions. All converters used in solar applications must have a high step-up capacity. A comparison of the suggested topology's voltage gain to that of existing transformerless topologies can be seen in Fig.12. On this graph, the voltage gain from all converters with varied duty cycles is shown. Out of all the provided converters, the conventional boost converter has the weakest boosting capacity, whereas the suggested converter has the biggest gain of the alternative topologies.

5. Conclusion

High-gain transformerless dc/dc converter design for usage in renewable energy systems is the topic of this article. There is a new configuration with an extra step. The designed setup had respectable efficiency with impressive step-up capability. The converter's operating principle and analytical analysis are shown and investigated in depth. We've successfully implemented a prototype in the lab. Researchers have examined a variety of use situations to verify the converter's boosting capacity and efficiency. In the literature, you may find a thorough analysis of the suggested configurations in relation to alternative transformerless topologies. The theory is supported by the experiments.

Conflict of interest statement

Authors declare that they do not have any conflict of interest.

References

[1] F. Blaabjerg and D. M. Ionel, ``Renewable energy devices and systems_State-of-the-art technology, research and development, challenges and future trends,'' Electr. Power Compon. Syst., vol. 43, no. 12, pp. 1319_1328, Jul. 2015.

[2] Li,W.; He, X. Review of nonisolated high-step-up DC/DC converters in photovoltaic grid-connected applications. IEEE Trans. Ind. Electron. 2011, 58, 1239–1250. [CrossRef]

[3] Souza, L.C.; Morais, D.C.; Silva, L.D.S.D.C.E.; Seixas, F.J.M.D.; Arenas, L.D.O. DC-DC 3SSC-a-based boost converter: Analysis, design, and experimental validation. Energies 2021, 14, 6771. [CrossRef]

[4] Gholizadeh, H.; Gorji, S.A.; Afjei, E.; Sera, D. Design and implementation of a new cuk-based step-up DC–DC converter. Energies 2021, 14, 6975. [CrossRef]
[5] Chub, A.; Vinnikov, D.; Blaabjerg, F.; Peng, F.Z. A review of galvanically isolated impedance-source DC-DC converters. IEEE Trans. Power Electron. 2016, 31, 2808–2828. [CrossRef]
[6] Abdel-Rahim, O.; Wang, H. A new high gain DC-DC converter with model-predictive-control based MPPT technique forphotovoltaic systems. CPSS Trans. Power Electron. Appl. 2020, 5, 191–200. [CrossRef]
[7] Arango, E.; Ramos-Paja, C.A.; Calvente, J.; Giral, R.; Serna-Garces, S.I. Asymmetrical interleaved dc/dc switching converters for photovoltaic and fuel cell applications—Part 2: Control-oriented models. Energies 2013, 6, 5570–5596. [CrossRef]
[8] Abdel-Rahim, O.; Chub, A.; Blinov, A.; Vinnikov, D. New high-gain non-inverting buck-boost converter. In Proceedings of the IECON 2021–47th Annual Conference of the IEEE Industrial Electronics Society, Toronto, ON, Canada, 13 October 2021; pp. 1–6.
[9] Ojeda-Rodríguez, Á.; González-Vizuete, P.; Bernal-Méndez, J.; Martín-Prats, M.A. A survey on bidirectional dc/dc power converter topologies for the future hybrid and all electric aircrafts. Energies 2020, 13, 4883. [CrossRef]
[10] De Souza, A.F.; Tofoli, F.L.; Ribeiro, E.R. Switched capacitor dc-dc converters: A survey on the main topologies, design characteristics, and applications. Energies 2021, 14, 2231. [CrossRef]
[11] Forouzesh, M.; Siwakoti, Y.P.; Gorji, S.A.; Blaabjerg, F.; Lehman, B. Step-up DC-DC converters: A comprehensive review of voltage-boosting techniques, topologies, and applications. IEEE Trans. Power Electron. 2017, 32, 9143–9178. [CrossRef]
[12] Andrade, A.M.S.S.; Martins, M.L.D.S. Quadratic-boost with stacked zeta converter for high voltage gain applications. IEEE J.Emerg. Sel. Top. Power Electron. 2017, 5, 1787–1796. [CrossRef]
[13] Ai, J.; Lin, M. Ultralarge gain step-up coupled-inductor dc-dc converter with an asymmetric voltage multiplier network for a sustainable energy system. IEEE Trans. Power Electron. 2017, 32, 6896–6903. [CrossRef]
[14] Vighetti, S.; Ferrieux, J.P.; Lembeye, Y. Optimization and design of a cascaded DC/DC converter devoted to grid-connected photovoltaic systems. IEEE Trans. Power Electron. 2012, 27, 2018–2027. [CrossRef]
[15] Zhang, Y.; Gao, Y.; Zhou, L.; Sumner, M. A switched-capacitor bidirectional dc-dc converter with wide voltage gain range for electric vehicles with hybrid energy sources. IEEE Trans. Power Electron. 2018, 33, 9459–9469. [CrossRef]
[16] Ballo, A.; Grasso, A.D.; Palumbo, G.; Tanzawa, T. Linear distribution of capacitance in Dickson charge pumps to reduce rise time. Int. J. Circ. Theor. Appl. 2020, 48, 555–566. [CrossRef]
[17] Ballo, A.; Grasso, A.D.; Palumbo, G. A simple and effective design strategy to increase power conversion efficiency of linear charge pumps. Int. J. Circ. Theor. Appl. 2020, 48, 157–161. [CrossRef]
[18] Ahmed, M.E.; Orabi, M.; AbdelRahim, O.M. Two-stage micro-grid inverter with high-voltage gain for photovoltaic applications. IET Power Electron. 2013, 6, 1812–1821. [CrossRef]
[19] Axelrod, B.; Berkovich, Y.; Ioinovici, A. Switched-capacitor/switched-inductor structures for getting transformerless hybrid DC–DC pwm converters. IEEE Trans. Circuits Syst. 2008, 55, 687–696. [CrossRef]
[20] Young, C.-M.; Chen, M.-H.; Chang, T.-A.; Ko, C.-C.; Jen, K.-K. Cascade Cockcroft–Walton Voltage Multiplier Applied to Transformerless High Step-Up DC–DC Converter. IEEE Trans. Ind. Electron. 2013, 60, 523–537. [CrossRef]
[21] Andrade, A.M.S.S.; Hey, H.L.; Schuch, L.; da Silva Martins, M.L. Comparative Evaluation of Single Switch High-Voltage Step-Up Topologies Based on Boost and Zeta PWM Cells. IEEE Trans. Ind. Electron. 2018, 65, 2322–2334. [CrossRef]
[22] Li, W.; Xiang, X.; Li, C.; Li, W.; He, X. Interleaved high step-up ZVT converter with built-in transformer voltage doubler cell for distributed PV generation system. IEEE Trans. Power Electron. 2013, 28, 300–313. [CrossRef]
[23] Liu, H.; Li, F. A novel high step-up converter with a quasi-active switched-inductor structure for renewable energy systems. IEEE Trans. Power Electron. 2016, 31, 5030–5039.
[24] De Paula, W.J.; Júnior, D.D.O.; Pereira, D.D.; Tofoli, F.L. Survey on non-isolated high-voltage step-up dc–dc topologies based on the boost converter. IET Power Electron. 2015, 8, 2044–2057.
[25] Stauth, J.T.; Seeman, M.D.; Kesarwani, K. Resonant switched-capacitor converters for sub-module distributed photovoltaic power management. IEEE Trans. Power Electron. 2013, 28, 1189–1198.
[26] Waradzyn, Z.; Stala, R.; Mondzik, A.; Penczek, A.; Skala, A.; Pirog, S. Efficiency Analysis of MOSFET-Based Air-Choke Resonant DC–DC Step-Up Switched-Capacitor Voltage Multipliers. IEEE Trans. Ind. Electron. 2017, 64, 8728–8738. [CrossRef]
[27] Cervera, A.; Evzelman, M.; Peretz, M.M.; Ben-Yaakov, S. A high-efficiency resonant switched capacitor converter with continuous conversion ratio. IEEE Trans. Power Electron. 2015, 30, 1373–1382.

[28] Stala, R.;Waradzyn, Z.; Mondzik, A.; Penczek, A.; Skała, A. DC–DC high step-up converter with low count of switches based on resonant switched-capacitor topology. In Proceedings of the 2019 21st European Conference on Power Electronics and Applications (EPE'19 ECCE Europe), Genova, Italy, 2–5 September 2019; pp. P.1–P.10.

[29] Shoyama, M.; Naka, T.; Ninomiya, T. Resonant switched capacitor converter with high efficiency. In Proceedings of the 2004 IEEE 35th Annual Power Electronics Specialists Conference 2004, Aachen, Germany, 20–25 June 2004; Volume 5, pp. 3780–3786.

[30] Kesarwani, K.; Sangwan, R.; Stauth, J.T. Resonant-switched capacitor converters for chip-scale power delivery: Design and implementation. IEEE Trans. Power Electron. 2015, 30, 6966–6977.

[31] Moulali, S., Vijay Muni, T., Bala Subrahmanyam, Y., & Kesav, S. (2018). A flying capacitor multilevel topology for pv system with apod and pod pulse width modulation. Journal of Advanced Research in Dynamical and Control Systems, 10(2), 96–101.

[32] Srikanth, M., Vijay Muni, T., VishnuVardhan, M., & Somesh, D. (2018). Design and simulation of PV-wind hybrid energy system. Journal of Advanced Research in Dynamical and Control Systems, 10(4), 999–1005.

[33] Vijay Muni, T., Sai Sri Vidya, G., & Rini Susan, N. (2017). Dynamic modeling of hybrid power system with mppt under fast varying of solar radiation. International Journal of Applied Engineering Research, 12(Special Issue 1), 530–537.

[34] Sudharshan Reddy, K., Sai Priyanka, A., Dusarlapudi, K., & Vijay Muni, T. (2019). Fuzzy logic based iUPQC for grid voltage regulation at critical load bus. International Journal of Innovative Technology and Exploring Engineering, 8(5), 721–725.

[35] Ilahi, S., Ramaiah, M. S., Muni, T. V., & Naidu, K. G. (2018). Study the performance of solar PV array under partial shadow using DC- DC converter. Journal of Advanced Research in Dynamical and Control Systems, 10(4 Special Issue), 1006–1014.